# Geometric and Electronic Structures of $Os_3(CO)_9(\mu_3\text{-}\eta^2,\eta^2,\eta^2\text{-}C_{60})$, $Os_3(CO)_8(P(CH_3)_3)(\mu_3\text{-}\eta^2,\eta^2,\eta^2\text{-}C_{60})$, and Their Anions ($Q = -1$ to $-4$): Reduction-Induced Conversion of $\pi$ to $\sigma$ $C_{60}$−Metal Complexes

Kyoung Hoon Kim, Jaehoon Jung, and Young-Kyu Han*

*Computational Chemistry Laboratory, Corporate R&D, LG Chem. Ltd. Research Park, Daejon, 305-380, Korea*

*Received February 12, 2004*

The geometries and electronic structures of $Os_3(CO)_9(\mu_3\text{-}\eta^2,\eta^2,\eta^2\text{-}C_{60})$ (OsF1), $Os_3(CO)_8(P(CH_3)_3)(\mu_3\text{-}\eta^2,\eta^2,\eta^2\text{-}C_{60})$ (OsF2), and their mono-, di-, tri-, and tetra-anions were calculated using a density functional method. Our calculations show that all three Os atoms are coordinated to $C_{60}$ in a $\pi$-type mode for the mono- and dianions, as well as in the neutral OsF1 and OsF2 complexes, but that third and fourth electron reductions form mixed $\sigma-\pi$-type coordinated compounds. A third electron reduction produces the $Os_3(CO)_9(\mu_3\text{-}\eta^2,\eta^2,\eta^1\text{-}C_{60})^{3-}$ and $Os_3(CO)_8(P(CH_3)_3)(\mu_3\text{-}\eta^2,\eta^2,\eta^1\text{-}C_{60})^{3-}$ complexes, while a fourth electron reduction produces the $Os_3(CO)_9(\mu_3\text{-}\eta^2,\eta^1,\eta^1\text{-}C_{60})^{4-}$ and $Os_3(CO)_8(P(CH_3)_3)(\mu_3\text{-}\eta^2,\eta^2,\eta^1\text{-}C_{60})^{4-}$ complexes. Our reduction potentials are calculated, in qualitatively good agreement with experimental data obtained using cyclic voltammetry.



## Introduction

The study of the chemical and physical properties of fullerenes is a dynamic field of research,[1] and there has been considerable interest in the anions of $C_{60}$[2,3] and exohedral metallofullerenes.[4−9] Understanding the effect of the metal substituent on the redox properties of $C_{60}$ is crucial for the development of specific electronic and optical applications, and the binding of $C_{60}$ to inorganic fragments has also demonstrated the remarkable versatility of this fullerene in its reactions with organometallic species.

In fullerene-metal cluster complexes, the exohedral metallofullerene chemistry is dominated by $\pi$-type $C_{60}$−metal bonds, as it has an $\eta^2$-$C_{60}$ bonding mode with most metals[5] and $\mu\text{-}\eta^2,\eta^2$-$C_{60}$ bonding modes for bimetallic $Re_2$, $Ru_2$, and $Ir_2$.[6] Some transition metals are known to interact with the sprayed $\pi$-orbitals of fullerene five- and six-membered rings.[7] Various $C_{60}$−metal cluster complexes[8] have been prepared, and a variety of cluster frameworks shown to bind to $C_{60}$ via a face-capping cyclohexatriene-like bonding mode, $\mu_3\text{-}\eta^2,\eta^2,\eta^2$-$C_{60}$. Recently, Park et al.[9] reported the first example of a ligand-induced conversion of a $\pi$ to $\sigma$ $C_{60}$−metal complex. They demonstrated the transformation of the bonding mode of $C_{60}$ on an $Os_3$ framework, from the $\mu_3\text{-}\eta^2,\eta^2,\eta^2$ bonding mode to the $\mu_3\text{-}\eta^1,\eta^2,\eta^1$ bonding mode that was induced by an external ligand.

In our study, we performed density functional calculations on neutral and variable anions ($Q = -1$ to $-4$) of $C_{60}$, $Os_3(CO)_9(\mu_3\text{-}\eta^2,\eta^2,\eta^2\text{-}C_{60})$ (OsF1), and $Os_3(CO)_8(P(CH_3)_3)(\mu_3\text{-}\eta^2,\eta^2,\eta^2\text{-}C_{60})$ (OsF2) (see Figure 1) to examine their structures, electrochemical properties, and the bonding modes between the metal cluster and the $C_{60}$. Park et al.[8a] have reported the synthesis and

* Corresponding author. E-mail: ykhan@lgchem.com. Fax: 82-42-863-7466.

(1) (a) Sawamura, M.; Kawai, K.; Matsuo, Y.; Kanie, K.; Kato, T.; Nakamura, E. *Nature* **2002**, *419*, 702. (b) Arvanitidis, J.; Papagelis, K.; Margadonna, S.; Prassides, K.; Fitch, A. N. *Nature* **2003**, *425*, 599 (c) Reed, C. A.; Kim, K.-C.; Bolskar, R. D.; Mueller, L. J. *Science* **2000**, *289*, 101. (d) Jarrold, M. F. *Nature* **2000**, *407*, 26. (e) Health, J. R. *Nature* **1998**, *393*, 730. (f) Becker, L.; Poreda, R. J.; Bada, J. L. *Science* **1996**, *272*, 249.

(2) (a) Fowler, P. W.; Ceulemans, A. *J. Phys. Chem.* **1995**, *99*, 508. (b) Larsson, S.; Volosov, A.; Rosen, A. *Chem. Phys. Lett.* **1987**, *137*, 501. (c) Haddon, R. C.; Brus, L. E.; Raghavachari, K. *Chem. Phys. Lett.* **1986**, *125*, 459. (d) Yang, S. H.; Pettiette, C. L.; Conceicao, J.; Cheshnovsky, O.; Smalley, R. E. *Chem. Phys. Lett.* **1987**, *139*, 233. (e) Brink, C.; Andersen, L. H.; Hvelplund, P.; Mathur, D.; Voldstad, J. D. *Chem. Phys. Lett.* **1995**, *233*, 52.

(3) (a) David, W. I. F.; Ibberson, R. M.; Matthewman, J. C.; Prassides, D.; Dennis, T. J. S.; Hare, J. P.; Kroto, H. W.; Taylor, R.; Wlaton, D. R. M. *Nature* **1991**, *353*, 147 (b) Yannoni, C. S.; Bernier, P. P.; Bethune, D. S.; Meijer, G.; Salem, J. R. *J. Am. Chem. Soc.* **1991**, *113*, 3190.

(4) (a) Hawkins, J. M.; Meyer, S.; Lewus, T. A.; Loren, S.; Hollander, F. J. *Science* **1991** *252*, 312. (b) Koga, N.; Morokuma, K. *Chem. Phys. Lett.* **1993** *202*, 330. (c) Fagan, P. J.; Calabrese, J. C.; Malone, B. *J. Am. Chem. Soc.* **1991**, *113*, 9408. (d) Alemany, M. M. G.; Dieguez, O.; Rey, C.; Gallego, L. J. *J. Chem. Phys.* **2001**, *114*, 9371 (e) Lee, G.; Cho, Y.-J.; Park, B. K.; Lee, K.; Park, J. T. *J. Am. Chem. Soc.* **2003**, *125*, 13920.

(5) (a) Fagan, P. J.; Calabrese, J. C.; Malone, B. *Science* **1991**, *252*, 1160. (b) Koefod, R. S.; Hudgens, M. F.; Shapley, J. R. *J. Am. Chem. Soc.* **1991**, *113*, 8957. (c) Hsu, H.-F.; Du, Y.; Albrecht-Schmitt, T. E.; Wilson, S. R. *Organometallics* **1998**, *17*, 1756.

(6) (a) Rasinkangas, M.; Pakkanen, T. T.; Pakkanen, T. A.; Ahlgren, M.; Rouvinen, J. *J. Am. Chem. Soc.* **1993**, *115*, 4901. (b) Mavunkal, L. J.; Chi, Y.; Peng, S.-M.; Lee, G.-H. *Organometallics* **1995**, *14*, 4454. (c) Chernega, A. N.; Gren, M. L. H.; Haggitt, J.; Stephens, A. H. H. *J. Chem. Soc., Dalton Trans.* **1998** 755.

(7) (a) Jemmis, E. D.; Manoharan, M.; Sharma P. K. *Organometallics* **2000**, *19*, 1879 (b) Jemmis, E. D.; Parameswaran, P.; Anoop, A *Int. J. Quantum Chem.* **2003**, *95*, 810 (c) Jemmis, E. D.; Sharma P. K. *J. Mol. Graphics Modell.* **2001**, *19*, 256

(8) (a) Song, H.; Lee, K.; Park, J. T.; Choi, M. *Organometallics* **1998**, *17*, 4477. (b) Hsu, H.-F.; Shapley, J. R. *J. Organomet. Chem.* **2000**, *599*, 97. (c) Lynn, M. A.; Lichtenberger, D. L. *J. Cluster Sci.* **2000**, *11*, 169 (d) Hsu, H.-F.; Shapley, J. R. *J. Am. Chem. Soc.* **1996**, *118*, 9192.

(9) (a) Song, H.; Lee, K.; Lee, C. H.; Park, J. T.; Chang, H. Y.; Choi, M.-G. *Angew. Chem. Int. Ed.* **2001**, *40*, 1500 (b) Song, H.; Lee, C. H.; Lee, K.; Park, J. T. *Organometallics* **2002**, *21*, 2514. (c) Lee, K.; Song, H.; Park, J. T. *Acc. Chem. Res.* **2003**, *36*, 78.

10.1021/om049887o CCC: $27.50 
Publication on Web 07/08/2004

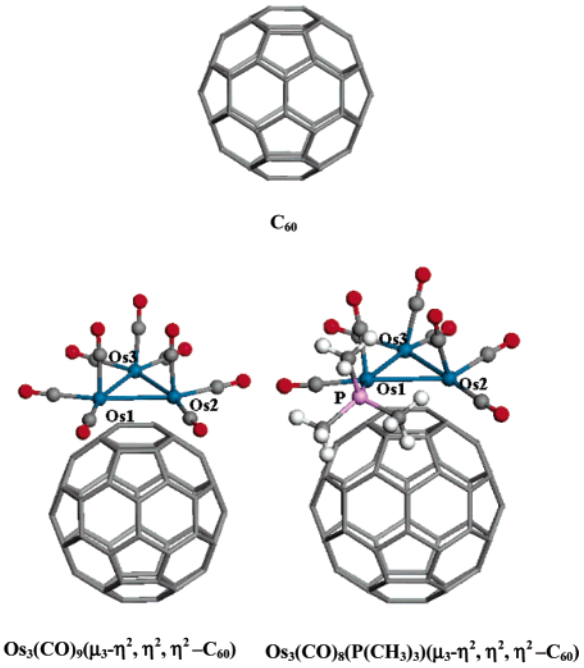


$Os_3(CO)_9(\mu_3\text{-}\eta^2,\eta^2,\eta^2\text{-}C_{60})$ $Os_3(CO)_8(P(CH_3)_3)(\mu_3\text{-}\eta^2,\eta^2,\eta^2\text{-}C_{60})$

**Figure 1.** Structures of $C_{60}$, $Os_3(CO)_9(\mu_3\text{-}\eta^2,\eta^2,\eta^2\text{-}C_{60})$-(OsF1), and $Os_3(CO)_8(P(CH_3)_3)(\mu_3\text{-}\eta^2,\eta^2,\eta^2\text{-}C_{60})$ (OsF2).

characterization of $\mu_3$-$\eta^2$, $\eta^2$, $\eta^2$-$C_{60}$ triosmium cluster complexes, OsF1 and OsF2, and electrochemical studies in 1,2-dichlorobenzene (DCB) solvent. The $Os_3$ core bonds symmetrically to a $C_6$ face of $C_{60}$, and each metal atom is bound in an $\eta^2$ fashion. To the best of our knowledge, there have been no theoretical or experimental studies on the geometries and electronic structures of metallofullerene anions. The optimized structures demonstrate that there are reduction-induced changes from $\pi$ to $\sigma$ bond type in the OsF1 and OsF2 complexes. Theoretical reduction potentials (RPs) for $C_{60}$, OsF1, OsF2, and their anions were calculated and compared with the available experimental RP values[8a] using cyclic voltammetry.

## Computational Section

Our calculations were based on the density functional theory (DFT) at the generalized gradient approximation (GGA) level (employing Becke's 1988 functional for exchange and Perdew and Wang's 1991 functional for correlation, BPW91[10]). The energy-adjusted relativistic effective core potential (RECP)[11] was used for the Os atoms. Double numerical plus polarization (DNP) basis sets were used for the C, H, O, and P atoms, and the valence electrons for Os were also expanded using the DNP basis set. All the structures of $C_{60}$, OsF1, OsF2, and their anions ($Q = -1$ to $-4$) as described were optimized without any symmetry restriction using the analytical gradients of the energies. To estimate higher accuracy molecular energies, relativistic all-electron Douglas−Kroll calculations[12] were performed on the RECP-optimized geometries. Calculations were performed on singlet and triplet states of $OsF1^{2-/4-}$ and $OsF2^{2-/4-}$ and doublet and quartet states of $OsF1^{3-}$ and $OsF2^{3-}$, as several spin states are possible for $OsF1^{2-/3-/4-}$ and $OsF2^{2-/3-/4-}$. The low spin states of OsF1 and OsF2 anions (singlet and doublet states, respectively) were calculated to be more stable, and these were used to obtain the electron affinity (EA) and RP values of OsF1 and OsF2, shown in Table 2. The solvation energies were calculated using the conductor-like screening model (COSMO),[13] to take into account bulk solvent effects. A dielectric constant value of $\epsilon = 7.5$ was employed in the Douglas−Kroll COSMO calculations, because DCB was used as the solvent in ref 7a. All the calculations were performed using the Dmol[3] software package.[14]

**Table 1. Calculated and Experimental Structural Parameters for $C_{60}$ and $Ru_3(CO)_9(\mu_3\text{-}\eta^2,\eta^2,\eta^2\text{-}C_{60})$ (bond lengths in Å)**

| | | calculation | experiment[a] |
|---|---|---|---|
| $C_{60}$ | [6,6][b] | 1.400 | 1.40 |
| | [6,5][c] | 1.453 | 1.45 |
| $Ru_3(CO)_9(\mu_3\text{-}\eta^2,\eta^2,\eta^2\text{-}C_{60})$ | Ru1−Ru2 | 2.913 | 2.8737 |
| | Ru1−Ru3 | 2.931 | 2.8790 |
| | Ru2−Ru3 | 2.942 | 2.8988 |
| | Ru1−C1 | 2.263 | 2.245 |
| | Ru1−C2 | 2.336 | 2.324 |
| | Ru2−C3 | 2.275 | 2.228 |
| | Ru2−C4 | 2.343 | 2.301 |
| | Ru3−C5 | 2.283 | 2.213 |
| | Ru3−C6 | 2.348 | 2.296 |
| | C1−C2 | 1.443 | 1.417 |
| | C2−C3 | 1.481 | 1.456 |
| | C3−C4 | 1.438 | 1.447 |
| | C4−C5 | 1.480 | 1.469 |
| | C5−C6 | 1.442 | 1.416 |
| | C6−C1 | 1.480 | 1.473 |

[a] Experimental values for $C_{60}$ are in ref 3, and those for $Ru_3(CO)_9(\mu_3\text{-}\eta^2,\eta^2,\eta^2\text{-}C_{60}$ in ref 8d. [b] The C−C bond corresponding to the fusion of two six-membered ring. [c] The C−C bond corresponding to the fusion of a six-membered ring and a five-membered ring.

**Table 2. Calculated Electron Affinities and Reduction Potentials (to the standard $Fc/Fc^+$ Scale) for $C_{60}$, OsF1, OsF2, and Their Anions ($Q = -1$ to $-4$)**

| | | | reduction potential | |
|---|---|---|---|---|
| | charge | electron affinity[a] | theory[b] | experiment[c] |
| $C_{60}$ | 0 | −1.24 | −1.24 | −1.08 |
| | −1 | −4.31 | −2.08 | −1.46 |
| | −2 | −7.43 | −2.96 | −1.90 |
| | −3 | −10.42 | −3.74 | −2.38 |
| OsF1 | 0 | −0.92 | −1.11 | −0.98 |
| | −1 | −3.67 | −1.89 | −1.33 |
| | −2 | −6.28 | −2.74 | −1.61 |
| | −3 | −8.78 | −3.38 | −1.74 |
| OsF2 | 0 | −1.15 | −1.25 | −1.06 |
| | −1 | −3.86 | −2.04 | −1.42 |
| | −2 | −6.54 | −2.98 | −1.93 |
| | −3 | −9.04 | −3.54 | −1.95 |

[a] Electron affinities were shifted so that the electron affinity of $C_{60}$ corresponds to the reduction potential of $C_{60}$. [b] Calculated reduction potentials on the ferrocene/ferrocenium ($Fc/Fc^+$) scale. [c] Experimental reduction potentials on the ferrocene/ferrocenium ($Fc/Fc^+$) scale examined by cyclic voltammetry.[8a]

(10) (a) Perdew, J. P.; Wang, Y. *Phys. Rev.* **1992**, *B45*, 13244. (b) Becke, A. D. *Phys. Rev.* **1988**, *A88*, 3098.
(11) (a) Dolg, M.; Wedig, U.; Stoll, H.; Preuss, H. *J. Chem. Phys.* **1987**, *86*, 866. (b) Bergner, A.; Dolg, M.; Kuechle, W.; Stoll, H.; Preuss, H. *Mol. Phys.* **1993**, *80*, 1431.
(12) (a) Douglas, M.; Kroll, N. M. *Ann. Phys. (NY)* **1974**, *82*, 89. (b) Hess, B. A. *Phys. Rev. A* **1985**, *32*, 756. (c) Hess, B. A. *Phys. Rev. A* **1986**, *33*, 3742. (d) Jansen, G.; Hess, B. A. *Phys. Rev. A* **1989**, *39*, 6016.
(13) Barone, V.; Cossi, M. *J. Phys. Chem. A* **1998**, *102*, 1995.
(14) (a) Delley, B. *J. Chem. Phys.* **1990**, *92*, 508. (b) Delley, B. *J. Chem. Phys.* **1991**, *94*, 7245. (c) Delley, B. *J. Chem. Phys.* **2000**, *113*, 7756. (d) Delley, B. *J. Phys. Chem.* **1996**, *100*, 6107.

## Results and Discussion

$C_{60}$, OsF1, OsF2, and their anions were optimized without any symmetry restriction, and we compared the optimized geometry parameters with the available experimental data.[3] We optimized the geometry parameters of OsF1 and OsF2 and wanted to compare their geometry parameters with any experimental results. Unfortunately, these have not been determined experimentally, and so the experimental geometry parameters of a complex analogous to OsF1, $Ru_3(CO)_9(\mu_3\text{-}\eta^2,\eta^2,\eta^2\text{-}C_{60})$,[8d] were compared with the calculated geometry parameters of $Ru_3(CO)_9(\mu_3\text{-}\eta^2,\eta^2,\eta^2\text{-}C_{60})$. Details on the geometries obtained are listed in Table 1. Comparison of the data indicates that our method is accurate enough to obtain the geometries of the metallofullerenes.

The optimized structures and the highest occupied molecular orbitals (HOMOs) for OsF1, OsF2, and their anions ($Q = -1$ to $-4$) are shown in Figure 2. The neutral OsF1 complex, as shown in Figure 2, has close to $C_{3v}$ symmetry, which agrees with the NMR spectrum.[8a] The $Os_3$ triangle is positioned centrally over a six-membered carbon ring ($C_6$-ring) in the $C_{60}$ moiety, and the two planes are nearly parallel as in $Ru_3(CO)_9(\mu_3\text{-}\eta^2,\eta^2,\eta^2\text{-}C_{60})$. The metal−metal bond lengths of OsF1 are longer than those of $Ru_3(CO)_9(\mu_3\text{-}\eta^2,\eta^2,\eta^2\text{-}C_{60})$ by about 0.05−0.07 Å. For both $Ru_3(CO)_9(\mu_3\text{-}\eta^2,\eta^2,\eta^2\text{-}C_{60})$ and OsF1, the $C_6$-ring of the $C_{60}$ moiety takes the form of cyclohexatriene, with each of its double bonds π-coordinated to a metal atom in an $\eta^2$ mode. The Ru−C bond distances show a short−long pattern at each metal center, with the average short distance being 2.273 Å and the average long distance being 2.342 Å. On the other hand, the Os atoms are located centrally over the double bonds of the $C_6$-ring with an average bond length being 2.339 Å. This is somewhat longer than the average Ru−C bond distance of 2.308 Å. OsF2, a trimethylphosphine-substituted complex, has the phosphine group located at an equatorial site and does not possess symmetry ($C_1$ point group). The $Os_3$ triangle is also positioned centrally over a $C_6$ ring in $C_{60}$, and each metal atom is coordinated to the double bonds of the $C_6$-ring in an $\eta^2$ mode.

The addition of electrons to the neutral complex changes the electronic structure and bond type of the Os−C[$C_{60}$] bond. A detailed representation of the changes in geometry is depicted in Figure 2, which shows top view geometries of the two $C_6$-rings: rings A and B, in the $C_{60}$ moiety of OsF1, OsF2, and their anions. Ring A is the six-membered carbon ring in the $C_{60}$ moiety over which the $Os_3$ triangle is coordinated, and ring B is the $C_6$-ring opposite ring A in the $C_{60}$ moiety. The circles on ring A denote the three Os atoms. In the neutral OsF1 and OsF2 complexes, the bond lengths of ring B are virtually identical to those of free $C_{60}$, while the bond lengths of ring A are longer than those of free $C_{60}$ by 0.028−0.056 Å, because of the π-type coordination to the Os atoms. The average Os−Os bond length ($r_{av}$[Os−Os]) is 2.995 Å. In the first and second electron reductions of OsF1, the changes in geometry of rings A and B are within 0.015 Å, and the three Os atoms remain π-coordinated to each of the three double bonds in ring A. All the Os−Os bond distances shrink slightly on the first and second electron reductions, and the $r_{av}$[Os−Os] value for the dianion of OsF1 is 2.975 Å.

Although both the first and second reductions slightly change the geometries of OsF1, the most notable change occurs after the third electron reduction. The Os3 atom of ring A is no longer π-coordinated to the $C_{60}$, but instead it binds to the C6 atom in a σ-type mode, while the Os1 and Os2 atoms remain π-coordinated to the (C1, C2) and (C3, C4) atoms, respectively. In this way, $Os_3(CO)_9(\mu_3\text{-}\eta^2,\eta^2,\eta^2\text{-}C_{60})^{2-}$ is transformed to $Os_3(CO)_9(\mu_3\text{-}\eta^2,\eta^2,\eta^1\text{-}C_{60})^{3-}$ by the third electron reduction. The C6 atom, which is bound to the Os atom in a σ-type mode, moves toward the Os atom. The sum of the three angles around the $sp^3$-hybridized C6 atom (330°) is considerably smaller than the sums of the angles of the other five carbon atoms (average = 350°) that possess $sp^2$ hybridization. The dihedral angles between the C1−C2−C5 plane and the C1−C5−C6 plane are 13° for $Os_3(CO)_9(\mu_3\text{-}\eta^2,\eta^2,\eta^1\text{-}C_{60})^{3-}$, while the corresponding dihedral angles for the neutral complexes and the mono- and dianions of OsF1 are less than 3°. The Os1−Os2 and Os1−Os3 bond lengths are also shortened by the third electron reduction, but the Os2−Os3 bond length becomes elongated from 2.975 Å to 3.004 Å. The HOMOs of the trianions of OsF1 clearly show that fractions of accepted electrons are present in the $Os_3(CO)_9$ moiety, unlike in the mono- and dianions, and the accepted electrons present in the $Os_3(CO)_9$ moiety contribute to the antibonding orbital of the Os2−Os3 bond. This results in its elongation. The tetra-anion of OsF1 remains a mixed σ−π-type compound, $Os_3(CO)_9(\mu_3\text{-}\eta^2,\eta^1,\eta^1\text{-}C_{60})^{4-}$. The Os2 and Os3 atoms are coordinated to the C3 and C6 atoms, respectively, in a σ-type fashion, and the Os1 atom is π-coordinated to the C1 and C2 atoms in an $\eta^2$ mode. The sum of the three angles around the $sp^3$-hybridized C3 and C6 atoms (330° and 331°, respectively) is considerably smaller than the sum of the angles around the other four $sp^2$-hybridized carbon atoms (average = 350°). The $sp^3$-hybridized C3 and C6 atoms are displaced from the smooth curvature of the $C_{60}$ ligand. The dihedral angle between the C2−C4−C5 plane and the C2−C3−C4 plane is 13°, and the dihedral angle between the C1−C2−C5 plane and the C1−C5−C6 plane is 16°. The Os2−Os3 bond length of OsF1 becomes extended, lengthening from 3.004 Å to 3.065 Å. HOMO distributions similar to those observed for the trianions are observed in the tetra-anions. The molecular orbital (MO) diagram for the neutral geometry of OsF1 is shown in Figure 3. The first two reductions are of the $C_{60}$ fragment, as the LUMO of OsF1 is nearly entirely $C_{60}$-based ($t_{1u}$). Therefore, the three Os atoms remain π-coordinated to each of the three double bonds in ring A. The LUMO+1 orbitals of OsF1 are formed from the LUMO of $Os_3(CO)_9$ and two of the LUMO($t_{1u}$) orbitals of $C_{60}$, which explains why the $Os_3(CO)_9$ moiety can accept electrons in the third and fourth reductions.

The changes in geometry of OsF2 on successive reductions are similar to those observed for OsF1. The OsF2 complex is also changed to a mixed σ−π-type compound, $Os_3(CO)_8(P(CH_3)_3)(\mu_3\text{-}\eta^2,\eta^2,\eta^1\text{-}C_{60})^{3-}$, by a third electron reduction. However, for the tetra-anions, the bonding modes of the $C_{60}$ moieties of OsF2 on the Os3 framework are different from those of OsF1. Unlike the $Os_3(CO)_9(\mu_3\text{-}\eta^2,\eta^1,\eta^1\text{-}C_{60})^{4-}$ complex, only the Os3 atom is coordinated to the C6 atom in a σ mode, and

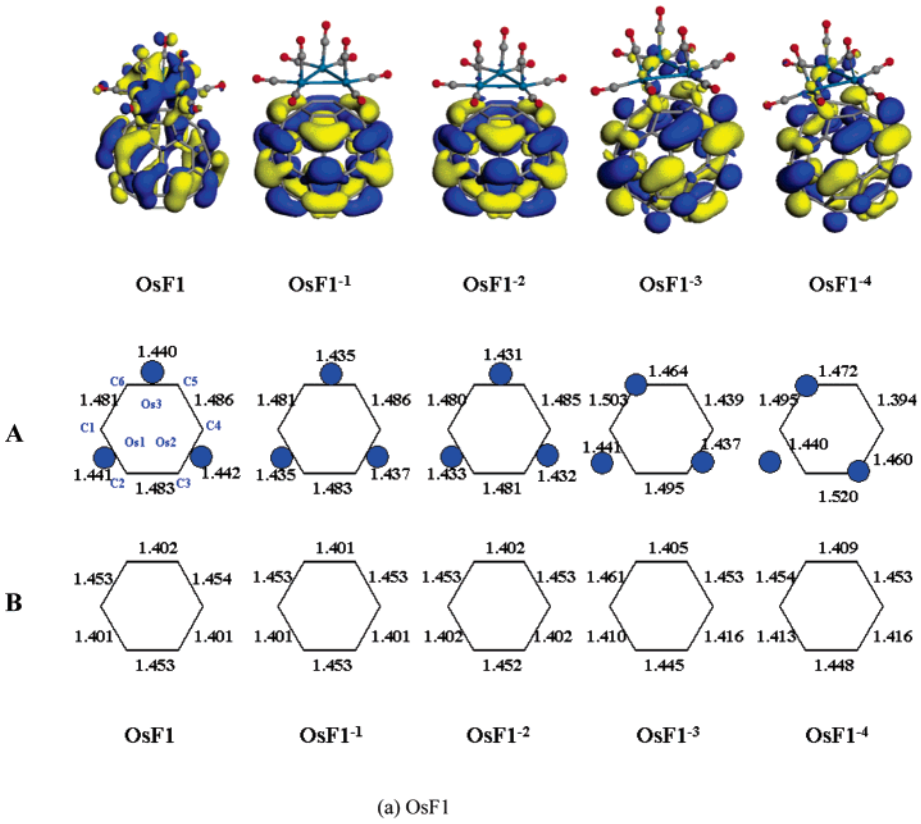


(a) OsF1

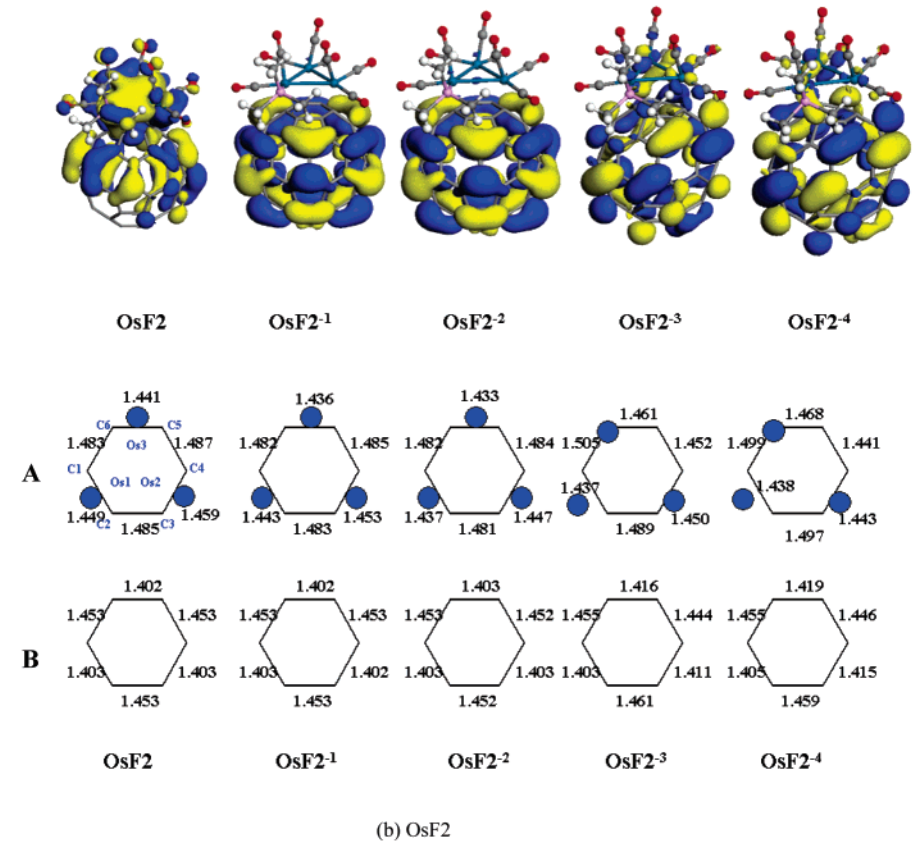


(b) OsF2

**Figure 2.** HOMO, optimized geometries, and $C_6$-rings in $C_{60}$ moiety of OsF1, OsF2, and their anions ($Q = -1$ to $-4$) (bond lengths are in Å).

the result is $Os_3(CO)_8(P(CH_3)_3)(\mu_3\text{-}\eta^2,\eta^2,\eta^1\text{-}C_{60})^{4-}$. This implies that the transformation of the bonding mode of $C_{60}$ from $\mu_3\text{-}\eta^2,\eta^1,\eta^1$ to $\mu_3\text{-}\eta^2,\eta^2,\eta^1$ can occur on an $Os_3$ framework by substituting a CO ligand with a $P(CH_3)_3$ ligand. It is not clear why this transformation occurs. However, we found that substitution of the CO ligand by the $P(CH_3)_3$ ligand elongates the Os1−Os2 bond length of the tetra-anion by 0.103 Å and the Os2−Os3

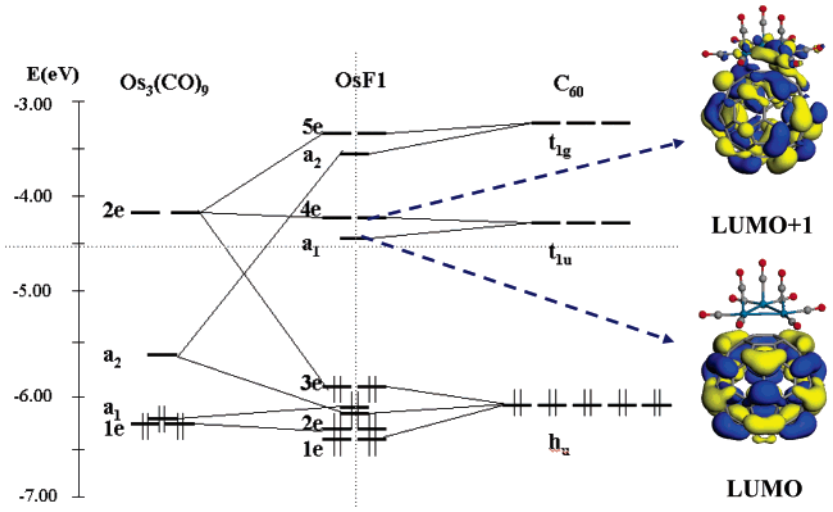


**Figure 3.** Molecular orbital diagrams for $Os_3(CO)_9(\mu_3\text{-}\eta^2,\eta^2,\eta^2\text{-}C_{60})$ and LUMO and LUMO+1 for $Os_3(CO)_9(\mu_3\text{-}\eta^2,\eta^2,\eta^2\text{-}C_{60})$.

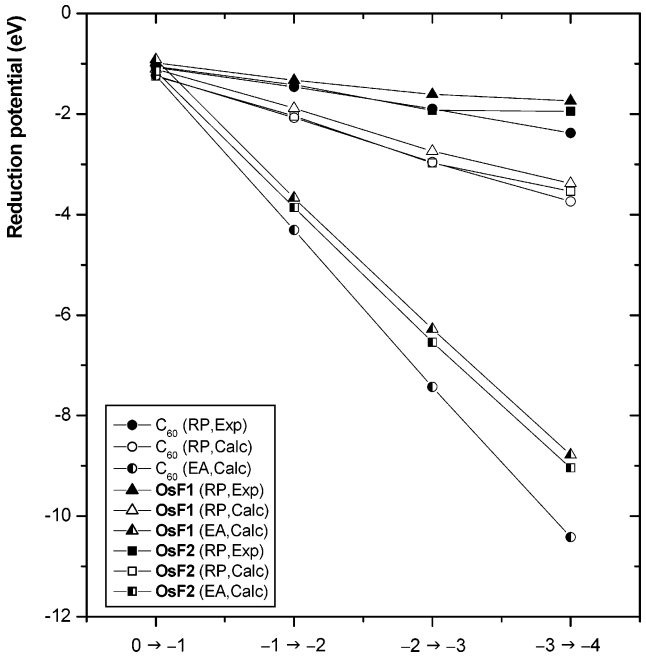


**Figure 4.** Calculated electron affinities, reduction potentials, and experimental reduction potentials (to the standard $Fc/Fc^+$ scale) of $C_{60}$, OsF1, OsF2, and their anions ($Q = -1$ to $-4$) (EA: electron affinity, RP: reduction potential, Calc: calculation, Exp: experiment).

and Os1−Os3 bond lengths by about 0.02 Å. For both OsF1 and OsF2, the geometry changes of ring B are not sensitive to electron reductions, and changes in the C−C bond lengths are less than 0.015 Å.

The calculated EA and RP values for $C_{60}$, OsF1, OsF2, and their anions ($Q = -1$ to $-4$) are listed in Table 2 along with the experimental cyclic voltammetric values, which are also depicted in Figure 4. The calculated RP values are, qualitatively, in good agreement with the experimental data if bulk solvent effects are taken into consideration. In the gas phase, OsF1 and OsF2 are more easily reduced than $C_{60}$. For example, the difference in EA values reaches 1.64 and 1.38 eV for the fourth electron reductions of OsF1 and OsF2, respectively. However, the experimental and theoretical RP values of OsF1 and OsF2 are close to those of $C_{60}$. Our calculations show that DCB stabilizes $C_{60}$ anions more than it does OsF1 and OsF2 anions (i.e., the difference in energy between $C_{60}$ anions in the gas phase and in DCB is greater than the difference in energy between OsF1 or OsF2 anions in the gas phase and in DCB). Therefore, the difference in the relative energies of $C_{60}$ and OsF1 or OsF2 is decreased. For example, in the gas phase, the OsF1 anion is more stable than the $C_{60}$ anion by 1.64 eV, but in DCB, the OsF1 anion is more stable than the $C_{60}$ anion by only 0.36 eV. The Os atoms in the OsF1 and OsF2 anions may not be 18-electron centers. However, OsF1 and OsF2 anions can exist as stable forms in DCB, because the solvent stabilizes the reduced complexes as shown in Figure 4. An analysis of the solvation energies shows that $C_{60}$, OsF1, and OsF2 anion complexes are stabilized by the electrostatic interactions between the metallofullerenes and the solvent molecules, in the order $C_{60} \gg$ OsF2 > OsF1. Details on the analysis of the solvation energies are shown in Table 1 of the Supporting Information.

## Conclusion

All three Os atoms are coordinated to the $C_6$–ring in a π-type mode for neutral and mono- and dianion complexes, but the products of the third and fourth electron reductions are mixed σ−π-type compounds. A third electron reduction produces $Os_3(CO)_9(\mu_3\text{-}\eta^2,\eta^2,\eta^1\text{-}C_{60})^{3-}$ and $Os_3(CO)_8(P(CH_3)_3)(\mu_3\text{-}\eta^2,\eta^2,\eta^1\text{-}C_{60})^{3-}$, and a fourth electron reduction produces $Os_3(CO)_9(\mu_3\text{-}\eta^2,\eta^1,\eta^1\text{-}C_{60})^{4-}$ and $Os_3(CO)_8(P(CH_3)_3)(\mu_3\text{-}\eta^2,\eta^2,\eta^1\text{-}C_{60})^{4-}$. We have demonstrated the first transformation of the bonding mode of $C_{60}$ from π to σ on an $Os_3$ framework solely induced by a change in electronic structure without modification of the ligand.

**Acknowledgment.** The authors are grateful to Prof. K. Lee and Dr. H. Song for helpful discussion.

**Supporting Information Available:** Structural parameters for $C_{60}$ and $Ru_3(CO)_9(\mu_3\text{-}\eta^2,\eta^2,\eta^2\text{-}C_{60})$, and solvation energies for $C_{60}$, OsF1, OsF2, and their anions are summarized. This material is available free of charge via the Internet at http://pubs.acs.org.

OM049887O